Nonlinear Impulsive Force on an Accelerating Container

Allen T. Chwang

K. H. Wang

Institute of Hydraulic Research,
The University of Iowa,
Iowa City, Iowa 52242

The nonlinear theory developed by Chwang [1] is applied to calculate the hydrodynamic pressure force on an accelerating rectangular or circular container. The fluid inside the container is initially at rest and the motion of the container is impulsive. During the initial stage of this impulsive motion, no travelling free-surface waves are present, and the fluid simply piles up on one side of the container and subsides on the opposite side. When the horizontal displacement of the container is small in comparison with the horizontal dimension of the container as well as the undisturbed fluid depth, the small-time expansion method is applied to obtain the velocity potential of the fluid which is accurate up to and including the third-order solution. The second-order free surface elevation is found to be singular along the contact line between the fluid and the container wall.

1 Introduction

The problem of determining the hydrodynamic force on an accelerated spacecraft tank filled with liquid propellant or on a fluid container in nuclear reactor installations due to earthquakes drew considerable attention of investigators in the past. Classical linear theory on this subject was successfully developed by Jacobsen [2] and Housner [3, 4]. The results obtained from the linearized theory were widely used by design engineers in aerospace engineering and in earthquake engineering. Recently Chwang [1] developed a two-dimensional nonlinear theory, based on the method of small-time expansions, to determine accurately the impulsive force on a suddenly moving vertical plate with the horizontal acceleration of the plate being expressed in a power series in time. The objective of the present paper is to apply Chwang's nonlinear theory to calculate the impulsive hydrodynamic pressure force on an accelerating rectangular or circular container.

The general problem of an accelerating container is formulated in section 2. Governing equations and boundary conditions for fluid inside a rigid, rectangular or circular container are presented. When the time t is much smaller than $(2h/a_1)^{1/2}$, where h is the undisturbed fluid depth and a_1 the characteristic acceleration magnitude, the velocity potential and the deviation of free surface are expanded in power series of t. The small time assumption is equivalent to the condition that the displacement of the fluid container, represented by $a_1 t^2/2$, is much smaller than the undisturbed fluid depth h. Analytical solution for a rectangular container is presented in section 3. Numerical results are given for the free surface profile, hydrodynamic pressure distribution and the total force on the container wall. Corresponding results for a circular container are presented in section 4.

Contributed by the Fluids Engineering Division of THE AMERICAN SOCIETY OF MECHANICAL ENGINEERS and presented at the Symposium on Rapid Fluid Transients in Fluid Structure Interactions, Houston, Texas, June 20-22, 1983. Manuscript received by the Fluids Engineering Division, February 8, 1983.

2 Governing Equations

We shall consider a container with a vertical side wall. The side boundary S_b of the container is given by

$$D(\mathbf{x},t)=0, \tag{1}$$

where $\mathbf{x} = (x,y)$ is a horizontal position vector and t denotes the time. The bottom of the container is at $z = 0$ and the undisturbed free surface of the fluid inside the container is at $z = h$, where z is the vertical axis pointing upwards. Initially the fluid and the container are at rest. At time $t = 0_+$, the container moves impulsively along the x direction with an acceleration

$$a_c(t) = \sum_{n=1}^{\infty} n\, a_n t^{n-1} \quad (a_1 \neq 0), \tag{2}$$

where a_n's are constant coefficients. The corresponding velocity and displacement of the container in the x-direction are

$$u_c(t) = \sum_{n=1}^{\infty} a_n t^n \tag{3}$$

and

$$s_c(t) = \sum_{n=1}^{\infty} \frac{a_n}{n+1} t^{n+1} \tag{4}$$

respectively. Due to this impulsive motion of the container, the fluid is set in motion and the disturbed free surface is at

$$z=h+\eta(\mathbf{x},t). \tag{5}$$

We assume that the fluid is incompressible and inviscid, and its motion is irrotational. Hence, the governing equation for the velocity potential $\phi(\mathbf{x}, z, t)$ is the Laplace equation

$$\nabla^2\phi=0. \tag{6}$$

At the bottom of the container,

$$\phi_z(\mathbf{x},0,t)=0, \tag{7}$$

where ϕ_z denotes $\partial\phi/\partial z$. On the side boundary S_b, the normal

velocity of the fluid must be the same as the normal velocity of the container. Thus

$$D_t + \mathbf{u} \cdot \nabla D = 0 \text{ on } S_b, \tag{8}$$

where $\mathbf{u} = \nabla\phi$ is the velocity vector of the fluid. The kinematic boundary condition on the free surface requires

$$\eta_t + (\nabla\phi)\cdot(\nabla\eta) = \phi_z \text{ at } z = h + \eta(\mathbf{x},t). \tag{9}$$

If we let the pressure on the free surface be zero, then the dynamic free surface condition is

$$\phi_t + \frac{1}{2}(\nabla\phi)\cdot(\nabla\phi) + g\eta = 0 \text{ at } z = h + \eta, \tag{10}$$

where g is the gravitational constant.

For small-time solutions valid when t is much smaller than $(2h/a_1)^{1/2}$, we expand the velocity potential and the deviation of free surface in power series of t as

$$\phi(\mathbf{x},z,t) = \sum_{n=1}^{\infty} t^n \phi_n(\mathbf{x},z), \tag{11}$$

$$\eta(\mathbf{x},t) = \sum_{n=1}^{\infty} t^n \eta_n(\mathbf{x}). \tag{12}$$

By equation (6) and equation (11), we have

$$\nabla^2 \phi_n(\mathbf{x},z) = 0 \ (n = 1,2,3, \ldots). \tag{13}$$

The bottom boundary condition (7) becomes

$$\frac{\partial \phi_n}{\partial z}(\mathbf{x},0) = 0 \ (n = 1,2,3, \ldots). \tag{14}$$

Substituting equation (11) and equation (12) into equation (9) and equation (10), and making Taylor series expansions about $z = h$, we obtain the free surface boundary conditions for $\phi_n(\mathbf{x}, h)$ $(n = 1,2,3, \ldots)$ as

$$\phi_1(\mathbf{x},h) = 0, \tag{15a}$$

$$\phi_2(\mathbf{x},h) = 0, \tag{15b}$$

$$\phi_3(\mathbf{x},h) = -\frac{g}{6}\frac{\partial \phi_1}{\partial z}(\mathbf{x},h) - \frac{1}{3}\left[\frac{\partial \phi_1}{\partial z}(\mathbf{x},h)\right]^2, \tag{15c}$$

and so on. The free surface elevations $\eta_n(\mathbf{x})$ $(n = 1,2,3, \ldots)$ are

$$\eta_1(\mathbf{x}) = 0, \tag{16a}$$

$$\eta_2(\mathbf{x}) = \frac{1}{2}\frac{\partial \phi_1}{\partial z}(\mathbf{x},h), \tag{16b}$$

$$\eta_3(\mathbf{x}) = \frac{1}{3}\frac{\partial \phi_2}{\partial z}(\mathbf{x},h), \tag{16c}$$

$$\eta_4(\mathbf{x}) = \frac{1}{4}\eta_2\frac{\partial^2 \phi_1}{\partial z^2}(\mathbf{x},h) + \frac{1}{4}\frac{\partial \phi_3}{\partial z}(\mathbf{x},h), \tag{16d}$$

and so on.

The hydrodynamic pressure p is related to the velocity potential ϕ through the Bernoulli equation

$$p = -\rho\left[\phi_t + \frac{1}{2}(\nabla\phi)\cdot(\nabla\phi)\right], \tag{17}$$

where ρ is the constant density of the fluid. If p is also expanded in a power series in t,

$$p(\mathbf{x},z,t) = \sum_{n=0}^{\infty} t^n p_n(\mathbf{x},z), \tag{18}$$

then by equation (11) and equation (17), we have

$$p_0(\mathbf{x},z) = -\rho\phi_1, \tag{19a}$$

$$p_1(\mathbf{x},z) = -2\rho\phi_2, \tag{19b}$$

$$p_2(\mathbf{x},z) = -\rho\left[3\phi_3 + \frac{1}{2}(\nabla\phi_1)\cdot(\nabla\phi_1)\right]. \tag{19c}$$

3 Rectangular Container

For a rectangular container with length L (in the x direction) and width B, the boundary condition on the side wall, given by equation (8), reduces to

$$\phi_x = u_c(t) \text{ at } x = s_c(t) \text{ and } x = L + s_c(t), \tag{20a}$$

$$\phi_y = 0 \text{ at } y = \pm B/2, \tag{20b}$$

where $u_c(t)$ and $s_c(t)$ are given by equation (3) and equation (4) respectively. Substituting equations (3), (4), and (11) into (20), we have

$$\frac{\partial \phi_n}{\partial y} = 0 \text{ at } y = \pm B/2 (n = 1,2,3, \ldots) \tag{21a}$$

and

$$\frac{\partial \phi_1}{\partial x} = a_1 \text{ at } x = 0 \text{ and } L, \tag{21b}$$

$$\frac{\partial \phi_2}{\partial x} = a_2 \text{ at } x = 0 \text{ and } L, \tag{21c}$$

$$\frac{\partial \phi_3}{\partial x} = a_3 - \frac{a_1}{2}\frac{\partial^2 \phi_1}{\partial x^2} \text{ at } x = 0 \text{ and } L, \tag{21d}$$

and so on.

Nomenclature

a_c = acceleration of a container
a_n = constant acceleration coefficients, see equation (2)
A_{ni} = constant coefficients, see equation (51)
b_i = constants, see equation (29c)
b_{ni} = eigenvalues, see equation (51e)
B = width of a rectangular container
B_{nm} = constant coefficients, see equation (49)
C_f = dimensionless force coefficient per unit length
C_F = dimensionless force coefficient
C_p = dimensionless pressure coefficient
D = boundary surface of a container
F = total force
g = gravitational constant
h = undisturbed fluid depth
I_n = modified Bessel function of the first kind, of order n
J_n = Bessel function of the first kind, of order n
k_m = constants, see equation (22b)
L = length of a rectangular container
p = pressure
r,θ = horizontal polar coordinates
r^* = radial position of container wall, see equation (38b)
R = constant radius of a circular container
R_n = pressure coefficients on the wall, see equation (33a)
s_c = displacement of a container
S_b = side boundary of a container
t = time
$\mathbf{u}$ = velocity vector of the fluid
u_c = velocity of a container
x,y = horizontal coordinates
z = vertical coordinate
α = intensity of acceleration
ϵ = dimensionless time, see equation (32)
η = deviation of free surface
η_n = surface expansion coefficients, see equation (12)
ρ = constant fluid density
ϕ = velocity potential of the fluid
ϕ_n = potential expansion coefficients, see equation (11)
ϕ_{31} = first part of the third-order potential
ϕ_{32} = second part of the third-order potential

The leading-order solution ϕ_1, satisfying equation (13) and the boundary conditions (14), (15a), (21a), and (21b), is obtained by the Fourier-series method as

$$\phi_1(\mathbf{x},z) = \frac{2a_1}{h} \sum_{m=1}^{\infty} \frac{(-1)^m \cos k_m z}{k_m^2 \sinh k_m L} \{\cosh[k_m(L-x)] - \cosh k_m x\}, \tag{22a}$$

where

$$k_m = \frac{(2m-1)\pi}{2h} \quad (m = 1,2,3, \ldots). \tag{22b}$$

From equations (16b) and (22), we have

$$\eta_2(\mathbf{x}) = \frac{a_1}{h} \sum_{m=1}^{\infty} \frac{\cosh[k_m(L-x)] - \cosh k_m x}{k_m \sinh k_m L}. \tag{23}$$

We note from equation (22) and equation (23) that these solutions do not depend on y, and in the limit as L goes to infinity they reduce to

$$\lim_{L\to\infty} \phi_1 = \frac{2a_1}{h} \sum_{m=1}^{\infty} \frac{(-1)^m}{k_m^2} \cos k_m z \, e^{-k_m x},$$

$$\lim_{L\to\infty} \eta_2 = \frac{a_1}{h} \sum_{m=1}^{\infty} k_m^{-1} e^{-k_m x},$$

which agree exactly with the solutions obtained by Chwang [1] for a semi-infinitely long channel.

The second-order solution can be obtained by the same method used for the first-order solution. Therefore

$$\phi_2(\mathbf{x},z) = \frac{2a_2}{h} \sum_{m=1}^{\infty} \frac{(-1)^m \cos k_m z}{k_m^2 \sinh k_m L} \{\cosh[k_m(L-x)] - \cosh k_m x\}, \tag{24}$$

$$\eta_3(\mathbf{x}) = \frac{2a_2}{3h} \sum_{m=1}^{\infty} \frac{\cosh[k_m(L-x)] - \cosh k_m x}{k_m \sinh k_m L}, \tag{25}$$

where k_m's are defined by equation (22b).

With the known solutions (22) and (24), equation (15c) becomes

$$\phi_3(\mathbf{x},h) = -\frac{ga_1}{3h} \sum_{m=1}^{\infty} \frac{\cosh[k_m(L-x)] - \cosh k_m x}{k_m \sinh k_m L} - \frac{4a_1^2}{3h^2} \left\{ \sum_{m=1}^{\infty} \frac{\cosh[k_m(L-x)] - \cosh k_m x}{k_m \sinh k_m L} \right\}^2, \tag{26}$$

and equation (21d) reduces to

$$\frac{\partial \phi_3}{\partial x}(0,y,z) = a_3 + \frac{a_1^2}{h} \sum_{m=1}^{\infty} (-1)^m \cos k_m z \frac{1-\cosh k_m L}{\sinh k_m L}, \tag{27a}$$

$$\frac{\partial \phi_3}{\partial x}(L,y,z) = a_3 - \frac{a_1^2}{h} \sum_{m=1}^{\infty} (-1)^m \cos k_m z \frac{1-\cosh k_m L}{\sinh k_m L}. \tag{27b}$$

To obtain the third-order solution ϕ_3, we first decompose it into two parts,

$$\phi_3(\mathbf{x},z) = \phi_{31}(\mathbf{x},z) + \phi_{32}(\mathbf{x},z), \tag{28}$$

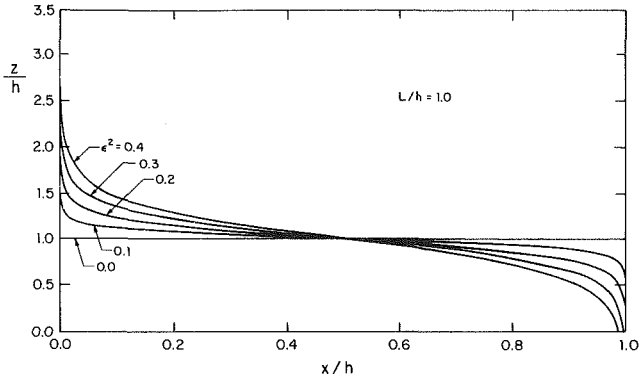

Fig. 1 Free surface profile at different values of ϵ

and require both parts to satisfy the Laplace equation (13). The boundary conditions for ϕ_{31} are the nonhomogeneous conditions (27a) and (27b), and the homogeneous conditions (14), (21a), and

$$\phi_{31}(\mathbf{x},h) = 0.$$

On the other hand, ϕ_{32} satisfies the nonhomogeneous condition (26) and the homogeneous conditions (14), (21a), and

$$\frac{\partial \phi_{32}}{\partial x}(0,y,z) = \frac{\partial \phi_{32}}{\partial x}(L,y,z) = 0.$$

The solutions ϕ_{31} and ϕ_{32} are then obtained by the Fourier-series method as

$$\phi_{31}(\mathbf{x},z) = \sum_{m=1}^{\infty} \frac{(-1)^m \cos k_m z}{k_m h \sinh k_m L} \left\{ \frac{2a_3}{k_m} (\cosh[k_m(L-x)] - \cosh k_m x) + a_1^2 (\sinh[k_m(L-x)] + \sinh k_m x) \right\}, \tag{29a}$$

$$\phi_{32}(\mathbf{x},z) = -\frac{4a_1^2}{3h^2} \sum_{m=1}^{\infty} \frac{1-\cosh k_m L}{k_m^3 L \sinh^2 k_m L} (k_m L - \sinh k_m L) + \frac{16a_1^2}{3h^2} \sum_{m=1}^{\infty} \sum_{n=m+1}^{\infty} (k_m^2 - k_n^2)^{-1} \left(\frac{1-\cosh k_n L}{k_n L \sinh k_n L} - \frac{1-\cosh k_m L}{k_m L \sinh k_m L} \right) + \frac{2a_1}{3h^2 L} \sum_{i=1}^{\infty} \frac{\cosh b_i z}{\cosh b_i h} \cos b_i x \left\{ -gh \sum_{m=1}^{\infty} \frac{1-(-1)^i}{k_m^2 + b_i^2} + 8a_1 \sum_{m=1}^{\infty} \frac{[1+(-1)^i](1-\cosh k_m L)}{(4k_m^2 + b_i^2) k_m \sinh k_m L} - 4a_1 \sum_{m=1}^{\infty} \sum_{n=m+1}^{\infty} \frac{[1+(-1)^i]}{k_m k_n \sinh k_m L \sinh k_n L} \left[\frac{k_m + k_n}{b_i^2 + (k_m + k_n)^2} (\sinh(k_m + k_n)L - \sinh k_m L - \sinh k_n L) \right.$$

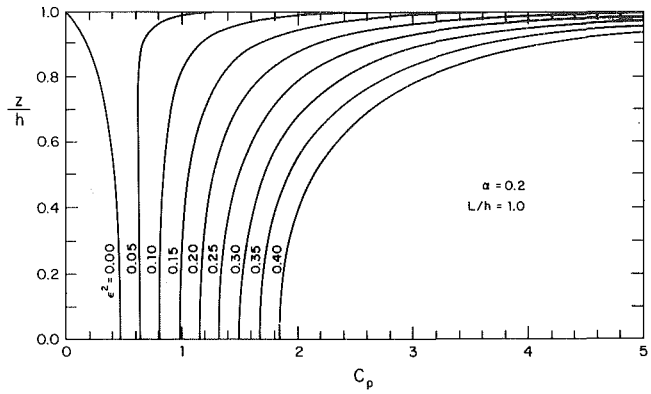

Fig. 2 The hydrodynamic pressure distribution on the wall at $\alpha = 0.2$, $L/h = 1.0$

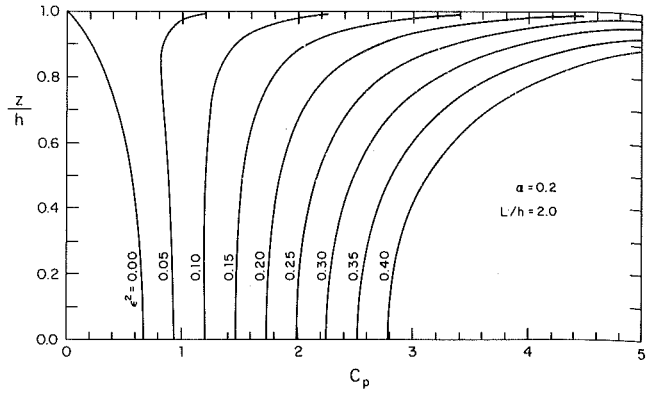

Fig. 3 The hydrodynamic pressure distribution on the wall at $\alpha = 0.2$, $L/h = 2.0$

$$+\frac{k_m-k_n}{b_i^2+(k_m-k_n)^2}(\sinh(k_m-k_n)L - \sinh k_mL+\sinh k_nL)\Big]\Big\}, \tag{29b}$$

where

$$b_i=\frac{i\pi}{L}\ (i=1,2,3,\ldots). \tag{29c}$$

To illustrate our analytical result, let us consider the case of a constant acceleration,

$$a_c(t)=a_1=\alpha g, \tag{30}$$

where α is the intensity of acceleration. By equations (5), (12), (16*a*), and (23), the disturbed free surface is at

$$\frac{z}{h}=1+2\epsilon^2\sum_{m=1}^{\infty}\frac{\cosh[k_m(L-x)]-\cosh k_mx}{k_mh\sinh k_mL}+0(\epsilon^4), \tag{31}$$

where ϵ is defined by

$$\epsilon=t(2h/a_1)^{-1/2}. \tag{32}$$

Figure 1 shows the free surface profile as computed from equation (31) for a rectangular container with length $L = h$. At $\epsilon = 0$, which corresponds to $a_1 = 0$ or $t = 0$, the free surface remains flat. As ϵ increases, the fluid inside the container piles up on the wall at $x = 0$ and subsides on the opposite side of the container. For non-vanishing values of ϵ, equation (31) has singularities at $x = 0$ and $x = L$ since the acceleration of the container is discontinuous at time $t = 0$. From equation (22), we also note that the vertical velocity of the fluid at the wall ($z = h$ and $x = 0$ or $x = L$) is singular. This singularity in vertical velocity and vertical acceleration at the free surface immediately adjacent to the wall exists even in the linear theory (Westergaard [6] and Housner [5]).

The hydrodynamic pressure distribution on the container wall at $x = s_c(t)$ can be expanded in a power series in t,

$$p(s_c(t),y,z,t)=\sum_{n=0}^{\infty}t^nR_n(y,z), \tag{33a}$$

where the R_n's are related to the p_n's by equation (4) and equation (18) as

$$R_0(y,z)=p_0(0,y,z), \tag{33b}$$

$$R_1(y,z)=p_1(0,y,z), \tag{33c}$$

$$R_2(y,z)=p_2(0,y,z)+\frac{a_1}{2}\frac{\partial p_0}{\partial x}(0,y,z), \tag{33d}$$

and so on. The nondimensional pressure defined by

$$C_p=\frac{p(s_c(t),y,z,t)}{\rho a_1h} \tag{34}$$

is obtained by equations (19), (22), (24), (29), and (33). Therefore

$$C_p=2\sum_{m=1}^{\infty}\frac{(-1)^m(1-\cosh k_mL)}{k_m^2h^2\sinh k_mL}\cos k_mz$$

$$+4\epsilon^2\Big\{\sum_{m=1}^{\infty}\frac{(-1)^{m+1}}{k_mh}\cosh k_mz$$

$$+\sum_{m=1}^{\infty}\frac{2(1-\cosh k_mL)}{k_m^3h^2L\sinh^2k_mL}(k_mL-\sinh k_mL)$$

$$+\sum_{m=1}^{\infty}\sum_{n=m+1}^{\infty}\frac{8}{(k_m^2-k_n^2)h^2}\Big[\frac{1-\cosh k_mL}{k_mL\sinh k_mL}$$

$$-\frac{1-\cosh k_nL}{k_nL\sinh k_nL}\Big]$$

$$+\sum_{i=1}^{\infty}\frac{\cosh b_iz}{\cosh b_ih}\Big[\sum_{m=1}^{\infty}\frac{1-(-1)^i}{\alpha hL(k_m^2+b_i^2)}$$

$$-8\sum_{m=1}^{\infty}\frac{(1+(-1)^i)(1-\cosh k_mL)}{k_mh^2L(4k_m^2+b_i^2)\sinh k_mL}$$

$$+\sum_{m=1}^{\infty}\sum_{n=m+1}^{\infty}\frac{4(1+(-1)^i)}{k_mk_nh^2L\sinh k_mL\sinh k_nL}$$

$$\Big(\frac{(k_m+k_n)(\sinh(k_m+k_n)L-\sinh k_mL-\sinh k_nL)}{(k_m+k_n)^2+b_i^2}$$

$$+\frac{(k_m-k_n)(\sinh(k_m-k_n)L-\sinh k_mL+\sinh k_nL)}{(k_m-k_n)^2+b_i^2}\Big)\Big]$$

$$-\Big[\sum_{m=1}^{\infty}\frac{(-1)^m}{k_mh}\cos k_mz\Big]^2$$

$$-\Big[\sum_{m=1}^{\infty}\frac{(-1)^m(1-\cosh k_mL)}{k_mh\sinh k_mL}\sin k_nz\Big]^2\Big\}+0(\epsilon^4). \tag{35}$$

The dimensionless pressure coefficient C_p is plotted in Fig. 2 versus the vertical depth for several different values of ϵ at $\alpha = 0.2$ and $L/h = 1.0$. We note from Fig. 2 that at fixed height, C_p increases with an increase in ϵ. From equation (32), we can interpret ϵ as the ratio of the horizontal displacement of the container, $a_1t^2/2$, to the undisturbed fluid depth h. Hence the larger the ratio ϵ is, the larger the pressure would be. For $\epsilon = 0$, C_p has a maximum value at the container

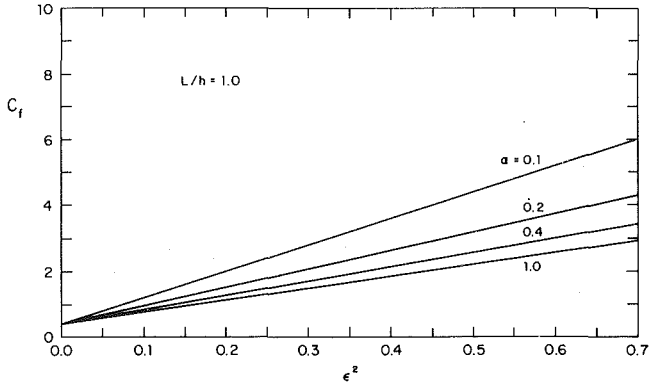

Fig. 4 The force coefficient C_f for various values of α at $L/h = 1.0$

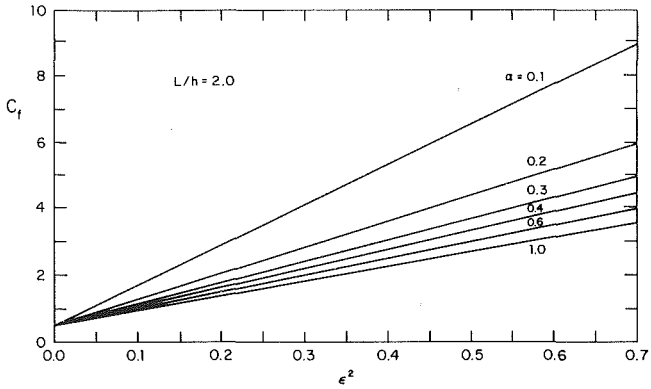

Fig. 5 The force coefficient C_f for various values of α at $L/h = 2.0$

bottom, it decreases monotonically as z increases. At the free surface $z = h$, C_p reduces to zero. For nonvanishing values of ϵ, C_p increases as z increases for large values of ϵ whereas it decreases at first, then increases as z approaches to the undisturbed free surface for small values of ϵ. At $z = h$, C_p becomes infinitely large since the free surface is at $z = h + \eta$ which is singular at the wall (see Fig. 1).

A similar diagram is shown in Fig. 3 for a longer container, $L/h = 2.0$. Comparing Fig. 2 with Fig. 3, we note that for same values of ϵ and z/h, C_p increases as the length L/h increases. As L/h approaches to infinity, C_p tends to the limiting distribution given by Chwang [1] as can be shown from equation (35).

The total horizontal hydrodynamic force on the container wall at $x = s_c(t)$ is obtained by integrating the pressure distribution. Hence, the dimensionless force coefficient per unit width defined by

$$C_f = \frac{1}{\rho\, a_1 h^2} \int_0^{h+\eta} p(s_c(t), y, z, t)\, dz, \tag{36}$$

follows from equations (19), (22), (23), (24), (29), and (33),

$$\begin{aligned} C_f = &-2 \sum_{m=1}^{\infty} \frac{1-\cosh k_m L}{k_m{}^3 h^3 \sinh k_m L} \\ &+ 4\epsilon^2 \Bigg\{ \frac{1}{2} \sum_{m=1}^{\infty} \frac{1}{k_m{}^2 h^2} \left[1 - \frac{(1-\cosh k_m L)^2}{\sinh^2 k_m L} \right] \\ &+ \sum_{m=1}^{\infty} \frac{2(1-\cosh k_m L)}{k_m{}^3 h^2 L \sinh^2 k_m L} (k_m L - \sinh k_m L) \\ &+ \sum_{m=1}^{\infty} \sum_{n=m+1}^{\infty} \frac{8}{(k_m^2 - k_n^2) h^2} \\ &\left[\frac{1-\cosh k_m L}{k_m L \sinh k_m L} - \frac{1-\cosh k_n L}{k_n L \sinh k_n L} \right] \\ &+ \sum_{i=1}^{\infty} \frac{\tanh b_i h}{b_i h} \Bigg[\sum_{m=1}^{\infty} \frac{1-(-1)^i}{\alpha h L (k_m{}^2 + b_i^2)} \\ &- 8 \sum_{m=1}^{\infty} \frac{(1+(-1)^i)(1-\cosh k_m L)}{k_m h^2 L (4k_m{}^2 + b_i^2) \sinh k_m L} \\ &+ \sum_{m=1}^{\infty} \sum_{n=m+1}^{\infty} \frac{4(1+(-1)^i)}{k_m k_n h^2 L \sinh k_m L \sinh k_n L} \\ &\Bigg(\frac{(k_m + k_n)(\sinh(k_m + k_n) L - \sinh k_m L - \sinh k_n L)}{(k_m + k_n)^2 + b_i^2} \\ &+ \frac{(k_m - k_n)(\sinh(k_m - k_n) L - \sinh k_m L + \sinh k_n L)}{(k_m - k_n)^2 + b_i^2} \Bigg) \Bigg] \Bigg\} \end{aligned} \tag{37}$$

with the terms of the order of $0(\epsilon^4)$ being neglected.

Figure 4 shows the force coefficient C_f versus ϵ for various values of α at $L/h = 1.0$. We note that for fixed values of α, C_f increases with ϵ. On the other hand, C_f decreases as α increases for fixed values of ϵ. At $\epsilon = 0$, C_f equals to 0.364 regardless of the values of α. A similar diagram is shown in Fig. 5 for $L/h = 2.0$. We note from Fig. 5 that at $\epsilon = 0$, C_f is equal to 0.499. In the limit as L/h approaches to infinity, C_f tends to 0.543 at $\epsilon = 0$. We also note from equation (37), Fig. 4 and Fig. 5 that although the hydrodynamic pressure on the wall is singular at $z = h$, this singularity is integrable. Therefore, the hydrodynamic force is regular on the wall.

4 Circular Container

For a circular container with radius R, equation (1) becomes

$$D = r - r^*(\theta, t) = 0, \tag{38a}$$

$$r^*(\theta, t) = s_c(t) \cos\theta + [R^2 - s_c^2(t) \sin^2\theta]^{1/2}, \tag{38b}$$

where r and θ are related to x and y by

$$x = r\cos\theta, y = r\sin\theta. \tag{39}$$

By means of equations (3), (4), (11), and (38), boundary condition (8) reduces to

$$\frac{\partial \phi_1}{\partial r}(R, \theta, z) = a_1 \cos\theta, \tag{40a}$$

$$\frac{\partial \phi_2}{\partial r}(R, \theta, z) = a_2 \cos\theta, \tag{40b}$$

$$\begin{aligned} \frac{\partial \phi_3}{\partial r}(R, \theta, z) = &\, a_3 \cos\theta - \frac{a_1}{2} \cos\theta \frac{\partial^2 \phi_1}{\partial r^2}(R, \theta, z) \\ &- \frac{a_1{}^2}{2R} \sin^2\theta - \frac{a_1}{2R^2} \sin\theta \frac{\partial \phi_1}{\partial \theta}(R, \theta, z), \end{aligned} \tag{40c}$$

and so on. By the Fourier-Bessel series method, the first-order solution of equation (13) satisfying the boundary conditions (14), (15a), and (40a) is

$$\phi_1(r, \theta, z) = \frac{2a_1 \cos\theta}{h} \sum_{m=1}^{\infty} \frac{(-1)^{m+1} I_1(k_m r)}{k_m{}^2 I_1'(k_m R)} \cos k_m z, \tag{41a}$$

where the k_m's are given by equation (22b), $I_1(k_m r)$ is the modified Bessel function of the first kind, of order one, and I_1' denotes

$$I_1'(x) = \frac{dI_1(x)}{dx} = I_0(x) - \frac{I_1(x)}{x}. \tag{41b}$$

From equation (16*b*) and equation (41), the leading-order surface deviation is

$$\eta_2(r,\theta) = -\frac{a_1 \cos\theta}{h} \sum_{m=1}^{\infty} \frac{I_1(k_m r)}{k_m I_1'(k_m R)}. \tag{42}$$

Similarly, the second-order solution is

$$\phi_2(r,\theta,z) = \frac{2a_2\cos\theta}{h} \sum_{m=1}^{\infty} \frac{(-1)^{m+1} I_1(k_m r)}{k_m^2 I_1'(k_m R)} \cos k_m z, \tag{43}$$

$$\eta_3(r,\theta) = -\frac{2a_2\cos\theta}{3h} \sum_{m=1}^{\infty} \frac{I_1(k_m r)}{k_m I_1'(k_m R)}. \tag{44}$$

Substituting equation (41*a*) and equation (43) into the free surface condition (15*c*), we have

$$\phi_3(r,\theta,h) = -\frac{4a_1^2\cos^2\theta}{3h^2}\left\{ \sum_{m=1}^{\infty} \frac{[I_1(k_m r)]^2}{k_m^2 [I_1'(k_m R)]^2} + 2\sum_{m=1}^{\infty}\sum_{n=m+1}^{\infty} \frac{I_1(k_m r) I_1(k_n r)}{k_m k_n I_1'(k_m R) I_1'(k_n R)} \right\}$$

$$+ \frac{g a_1 \cos\theta}{3h} \sum_{m=1}^{\infty} \frac{I_1(k_m r)}{k_m I_1'(k_m R)}. \tag{45}$$

By means of equation (41*a*) and equation (43), the boundary condition (40*c*) becomes

$$\frac{\partial \phi_3}{\partial r}(R,\theta,z) = a_3 \cos\theta - \frac{a_1^2}{2R}\sin^2\theta + a_1^2\cos^2\theta \sum_{m=1}^{\infty} \frac{(-1)^m I_1''(k_m R)}{h\, I_1'(k_m R)} \cos k_m z$$

$$- a_1^2 \sin^2\theta \sum_{m=1}^{\infty} \frac{(-1)^m I_1(k_m R)}{k_m^2 R^2 h I_1'(k_m R)} \cos k_m z, \tag{46a}$$

where

$$I_1''(x) = \left(1 + \frac{2}{x^2}\right) I_1(x) - \frac{I_0(x)}{x}. \tag{46b}$$

We now separate the third-order solution into two parts,

$$\phi_3(r,\theta,z) = \phi_{31}(r,\theta,z) + \phi_{32}(r,\theta,z), \tag{47}$$

each of which satisfies the Laplace equation (13). The boundary conditions for ϕ_{31} are the non-homogeneous condition (46) and the homogeneous conditions (14) and

$$\phi_{31}(r,\theta,h) = 0. \tag{48}$$

Therefore,

$$\phi_{31}(r,\theta,z) = \sum_{m=1}^{\infty} B_{0m} I_0(k_m r) \cos k_m z + \cos\theta \sum_{m=1}^{\infty} B_{1m} I_1(k_m r) \cos k_m z + \cos 2\theta \sum_{m=1}^{\infty} B_{2m} I_2(k_m r) \cos k_m z, \tag{49a}$$

where

$$B_{0m} = \frac{(-1)^{m+1} a_1^2}{2k_m^3 R^2 h I_1(k_m R) I_1'(k_m R)} [I_1(k_m R) - k_m^2 R^2 I_1''(k_m R) - k_m R\, I_1'(k_m R)], \tag{49b}$$

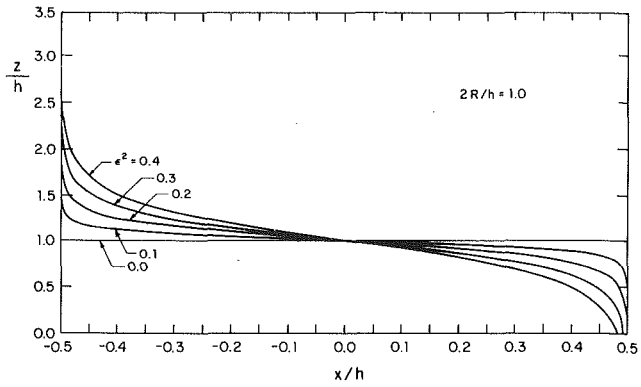

Fig. 6 Free surface profile at the central plane of a circular container

$$B_{1m} = \frac{2(-1)^{m+1} a_3}{k_m^2 h I_1'(k_m R)}, \tag{49c}$$

$$B_{2m} = \frac{(-1)^m a_1^2}{2k_m^3 R^2 h\, I_1'(k_m R) I_2'(k_m R)} [I_1(k_m R) + k_m^2 R^2 I_1''(k_m R) - k_m R\, I_1'(k_m R)], \tag{49d}$$

$$I_2'(x) = \left(1 + \frac{4}{x^2}\right) I_1(x) - \frac{2}{x} I_0(x). \tag{49e}$$

The boundary conditions to be satisfied by ϕ_{32} are equation (14), equation (45), and

$$\frac{\partial \phi_{32}}{\partial r}(R,\theta,z) = 0. \tag{50}$$

Hence

$$\phi_{32}(r,\theta,z) = \sum_{i=0}^{\infty} A_{0i} J_0(b_{0i} r) \cosh b_{0i} z + \cos\theta \sum_{i=1}^{\infty} A_{1i} J_1(b_{1i} r) \cosh b_{1i} z + \cos 2\theta \sum_{i=1}^{\infty} A_{2i} J_2(b_{2i} r) \cosh b_{2i} z, \tag{51a}$$

where

$$A_{0i} = \frac{-4a_1^2}{3h^2 R^2 J_0^2(b_{0i} R) \cosh b_{0i} h} \left\{ \sum_{m=1}^{\infty} \frac{1}{k_m^2 [I_1'(k_m R)]^2} \int_0^R r I_1^2(k_m r) J_0(b_{0i} r)\, dr + \sum_{m=1}^{\infty}\sum_{n=m+1}^{\infty} \frac{2}{k_m k_n I_1'(k_m R) I_1'(k_n R)} \int_0^R r I_1(k_m r) I_1(k_n r) J_0(b_{0i} r)\, dr \right\}, \tag{51b}$$

$$A_{1i} = \frac{2g a_1 b_{1i}^2}{3h(b_{1i}^2 R^2 - 1) J_1^2(b_{1i} R) \cosh b_{1i} h} \left\{ \sum_{m=1}^{\infty} \frac{1}{k_m I_1'(k_m R)} \int_0^R r I_1(k_m r) J_1(b_{1i} r)\, dr \right\}, \tag{51c}$$

$$A_{2i} = \frac{-4a_1^2 b_{2i}^2}{3h^2(b_{2i}^2 R^2 - 4) J_2^2(b_{2i} R) \cosh b_{2i} h}$$

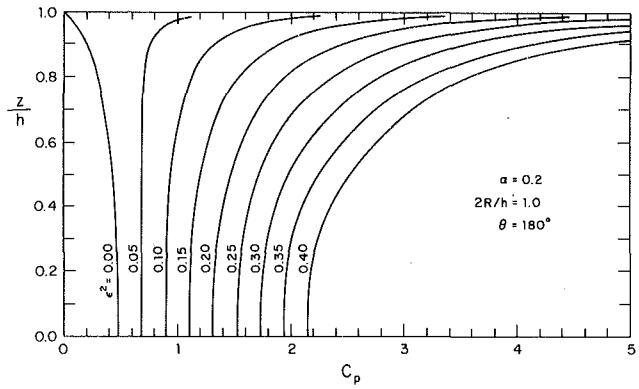

Fig. 7 The hydrodynamic pressure on a circular container at $\alpha = 0.2$, $2R/h = 1.0$, and $\theta = 180$ deg

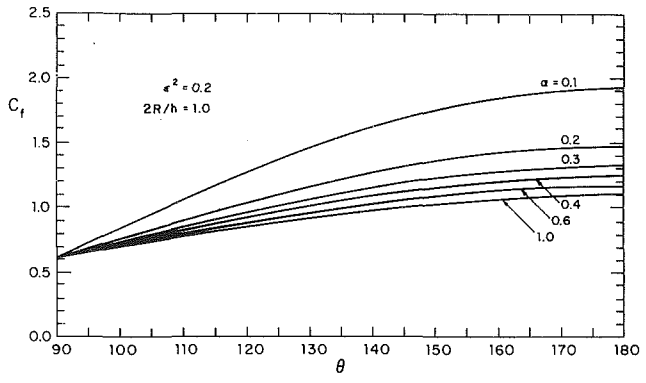

Fig. 8 The dimensionless force coefficient versus angular position at $\epsilon^2 = 0.2$ and $2R/h = 1.0$

$$\left\{ \sum_{m=1}^{\infty} \frac{1}{k_m^2 [I_1'(k_m R)]^2} \int_0^R r I_1^2(k_m r) J_2(b_{2i} r)\, dr \right.$$

$$+ \sum_{m=1}^{\infty} \sum_{n=m+1}^{\infty} \frac{2}{k_m k_n I_1'(k_m R) I_1'(k_n R)} \int_0^R r I_1(k_m r)$$

$$\left. I_1(k_n r) J_2(b_{2i} r)\, dr \right\}, \tag{51d}$$

$$J_n'(b_{ni} R) = 0 \quad (n = 0,1,2), \quad b_{00} = 0. \tag{51e}$$

We now consider the case of a constant acceleration, described by equation (30), to illustrate the analytical result. The free surface elevation, with terms of the order of $0(\epsilon^4)$ being neglected, is obtained by equations (5), (12), (16*a*), and (42),

$$\frac{z}{h} = 1 - 2\epsilon^2 \cos\theta \sum_{m=1}^{\infty} \frac{I_1(k_m r)}{k_m h I_1'(k_m R)}. \tag{52}$$

The free surface elevation at the central plane ($\theta = 0$ and $\theta = \pi$) as computed from equation (52) is shown in Fig. 6 for various values of ϵ at $2R/h = 1.0$. We note from Fig. 6 that at $\epsilon = 0$, the fluid surface remains horizontal inside the circular container. For nonvanishing values of ϵ, the free surface profile is similar to that inside a rectangular container. Comparing Fig. 6 with Fig. 1, we observe that the piling-up and subsiding phenomenon is more dominant in the case of a circular container. Along the container wall ($r = R$), the surface elevation is singular for nonvanishing values of ϵ.

The hydrodynamic pressure distribution on the container wall at $r = r^*(\theta, t)$ may be expressed in a power series in t,

$$p(r^*, \theta, z, t) = \sum_{n=0}^{\infty} t^n R_n(\theta, z). \tag{53a}$$

By equation (4), equation (18), and equation (38), we have

$$R_0(\theta, z) = p_0(R, \theta, z), \tag{53b}$$

$$R_1(\theta, z) = p_1(R, \theta, z), \tag{53c}$$

$$R_2(\theta, z) = p_2(R, \theta, z) + \frac{a_1}{2} \cos\theta \frac{\partial p_0}{\partial r}(R, \theta, z), \tag{53d}$$

and so on. The dimensionless pressure coefficient is thus obtained by equations (19), (41), (43), (49), (51), and (53) as

$$C_p = \frac{p(r^*, \theta, z, t)}{\rho a_1 h}$$

$$= 2 \cos\theta \sum_{m=1}^{\infty} \frac{(-1)^m I_1(k_m R)}{k_m^2 h^2 I_1'(k_m R)} \cos k_m z$$

$$+ 2\epsilon^2 \left\{ \cos^2\theta \sum_{m=1}^{\infty} \frac{(-1)^m \cos k_m z}{k_m h} \right.$$

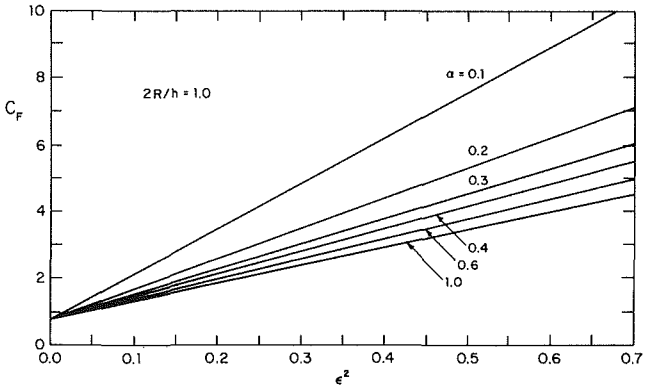

Fig. 9 The total force coefficient C_F versus ϵ^2 for various values of α at $2R/h = 1.0$

$$- 2 \cos^2\theta \left[\sum_{m=1}^{\infty} \frac{(-1)^m \cos k_m z}{k_m h} \right]^2$$

$$- 2 \sin^2\theta \left[\sum_{m=1}^{\infty} \frac{(-1)^m I_1(k_m R)}{k_m^2 R h I_1'(k_m R)} \cos k_m z \right]^2$$

$$- 2 \cos^2\theta \left[\sum_{m=1}^{\infty} \frac{(-1)^m I_1(k_m R)}{k_m h I_1'(k_m R)} \sin k_m z \right]^2$$

$$- \frac{3}{a_1^2} \sum_{m=1}^{\infty} [B_{0m} I_0(k_m R) + \cos 2\theta\, B_{2m} I_2(k_m R)] \cos k_m z$$

$$- \frac{3}{a_1^2} \sum_{i=0}^{\infty} A_{0i} J_0(b_{0i} R) \cosh b_{0i} z$$

$$- \frac{3\cos\theta}{a_1^2} \sum_{i=1}^{\infty} A_{1i} J_1(b_{1i} R) \cosh b_{1i} z$$

$$\left. - \frac{3\cos 2\theta}{a_1^2} \sum_{i=1}^{\infty} A_{2i} J_2(b_{2i} R) \cosh b_{2i} z \right\} + 0(\epsilon^4). \tag{54}$$

The dimensionless pressure coefficient C_p is shown in Fig. 7 for the case in which $\alpha = 0.2$, $2R/h = 1.0$, and $\theta = 180$ deg. Comparing Fig. 7 with Fig. 2, we note that when the diameter of a circular container is the same as the length of a rectangular container, C_p is larger for a circular container than that for a rectangular one with other parameters being kept at the same values. This means a circular container has more influence on the fluid motion inside it than a rectangular container has. The dimensionless force coefficient per unit arc length along the container wall, C_f, is obtained by integrating equation (54) with respect to z,

$$C_f(\theta) = \frac{1}{h}\int_0^{h+\eta} C_p(\theta,z)\,dz$$

$$= -2\cos\theta \sum_{m=1}^{\infty} \frac{I_1(k_mR)}{k_m^3 h^3 I_1'(k_mR)}$$

$$+2\epsilon^2\Bigg\{-\sum_{m=1}^{\infty}\frac{2\cos^2\theta}{k_m^2h^2} - \sum_{m=1}^{\infty}\frac{\sin^2\theta\, I_1^2(k_mR)}{k_m^4h^2R^2[I_1'(k_mR)]^2}$$

$$-\sum_{m=1}^{\infty}\frac{\cos^2\theta I_1^2(k_mR)}{k_m^2h^2[I_1'(k_mR)]^2}$$

$$+\sum_{m=1}^{\infty}\frac{3(-1)^m}{k_mha_1^2}[B_{0m}I_0(k_mR)+\cos 2\theta\, B_{2m}I_2(k_mR)]$$

$$-\sum_{i=0}^{\infty}\frac{3\sinh b_{0i}h}{b_{0i}h\,a_1^2}A_{0i}J_0(b_{0i}R)$$

$$-\sum_{i=1}^{\infty}\frac{3\cos\theta\sinh b_{1i}h}{b_{1i}h\,a_1^2}A_{1i}J_1(b_{1i}R)$$

$$-\sum_{i=1}^{\infty}\frac{3\cos 2\theta\sinh b_{2i}h}{b_{2i}h\,a_1^2}A_{2i}J_2(b_{2i}R)\Bigg\}$$

$$+0(\epsilon^4). \tag{55}$$

The numerical result for C_f obtained from equation (55) is shown in Fig. 8 versus the angular position from 90 to 180 deg at $\epsilon^2 = 0.2$ and $2R/h = 1.0$. We note from Fig. 8 that at a fixed angular position C_f decreases as α increases; whereas for fixed values of α, C_f decreases as the angle decreases from 180 to 90 deg. The total hydrodynamic pressure force on the circular container wall from $\theta = 90$ deg to $\theta = 270$ deg is

$$F = \rho a_1 R h^2 C_F, \tag{56a}$$

where C_F is related to C_f by

$$C_F = \int_{\pi/2}^{3\pi/2} C_f(\theta)\,d\theta. \tag{56b}$$

The total force coefficient C_F is plotted in Fig. 9 versus ϵ^2 for several fixed values of α at $2R/h = 1.0$. This figure is very similar to Fig. 4 and Fig. 5 for a rectangular container. At $\epsilon = 0$, $C_F = 0.762$ which is independent of the values of α. As R/h approaches to infinity, this value tends to 1.09 as computed from equation (55) and equation (56), which is twice the corresponding value for a rectangular container.

Acknowledgment

The authors are grateful to Professor John F. Kennedy for partial financial support. This work was originally sponsored by the National Science Foundation, under Grant CEE-8020564 A01.

References

1 Chwang, A. T., "Nonlinear Hydrodynamic Pressure on an Accelerating Plate," *Physics of Fluids*, Vol. 26, 1983, pp. 383–387.

2 Jacobsen, L. S., "Impulsive Hydrodynamics of Fluid Inside a Cylindrical Tank and of Fluid Surrounding a Cylindrical Pier," *Bull. Seism. Soc. Am.*, Vol. 39, 1949, pp. 189–204.

3 Housner, G. W., "Dynamic Pressures on Accelerated Fluid Containers," *Bull. Seism. Soc. Am.*, Vol. 47, No. 1, 1957, pp. 15–35.

4 Housner, G. W., "Dynamic Analysis of Fluids in Containers Subjected to Acceleration," in *"Nuclear Reactors and Earthquakes,"* TID-7021, U.S. Atomic Energy Commission, 1963, pp. 367–390.

5 Housner, G. W., "The Momentum-Balance Method in Earthquake Engineering," *Mechanics Today*, Vol. 5, 1980, pp. 113–127.

6 Westergaard, H. M., "Water Pressures on Dams During Earthquakes," *Trans. ASCE*, Vol. 98, 1933, pp. 418–433.